



HAL
open science

Quantifying suspended sediment sources during runoff events in headwater catchments using spectrocolorimetry

Cédric Legout, Jérôme Poulénard, Julien Nemery, Oldrich Navratil, Thomas Grangeon, O. Evrard, Michel Esteves

► **To cite this version:**

Cédric Legout, Jérôme Poulénard, Julien Nemery, Oldrich Navratil, Thomas Grangeon, et al.. Quantifying suspended sediment sources during runoff events in headwater catchments using spectrocolorimetry. *Journal of Soils and Sediments*, 2013, 13, p. 1478-1492. 10.1007/s11368-013-0728-9. halsde-00864710

HAL Id: halsde-00864710

<https://hal.science/halsde-00864710>

Submitted on 26 May 2020

HAL is a multi-disciplinary open access archive for the deposit and dissemination of scientific research documents, whether they are published or not. The documents may come from teaching and research institutions in France or abroad, or from public or private research centers.

L'archive ouverte pluridisciplinaire **HAL**, est destinée au dépôt et à la diffusion de documents scientifiques de niveau recherche, publiés ou non, émanant des établissements d'enseignement et de recherche français ou étrangers, des laboratoires publics ou privés.

1 SEDIMENTS, SEC 3 • HILLSLOPE AND RIVER BASIN SEDIMENT DYNAMICS • RESEARCH
2 ARTICLE

3

4 **Quantifying suspended sediment sources during runoff events in headwater catchments using**
5 **spectrocolorimetry**

6

7

8 **Cédric Legout • Jérôme Poulenard • Julien Nemery • Oldrich Navratil • Thomas Grangeon •**
9 **Olivier Evrard • Michel Esteves**

10

11 C. Legout (✉) • T. Grangeon

12 UJF-Grenoble 1 /CNRS / G-INP / IRD, LTHE UMR 5564, 38041 Grenoble, France

13 e-mail: cedric.legout@ujf-grenoble.fr

14

15 J. Poulenard

16 Université de Savoie, EDYTEM, Savoie Technolac, 73376 Le Bourget du Lac Cedex, France

17

18 J. Nemery

19 G-INP / UJF-Grenoble 1 / CNRS / IRD, LTHE UMR 5564, 38041 Grenoble, France

20

21 O. Navratil

22 Université de Lyon 2, EVS UMR 5600, avenue Pierre Mendès-France, 69676 Bron, France

23

24 O. Evrard

25 Laboratoire des Sciences du Climat et de l'Environnement (LSCE/IPSL), Unité Mixte de Recherche

26 8212 (CEA, CNRS, UVSQ), 91198-Gif-sur-Yvette Cedex, France

27

28 M. Esteves

29 IRD / UJF-Grenoble 1 / CNRS / G-INP, LTHE UMR 5564, 38041 Grenoble, France

30

31 (✉) **Corresponding author:**

32 Tel: +33 4 76 63 56 63

33 Fax: +33 4 76 82 50 01

34 e-mail: cedric.legout@ujf-grenoble.fr

35

36 **Abstract**

37 *Purpose* Increasing the understanding of the hydro-sedimentary dynamics at the catchment scale
38 requires high temporal resolution data on suspended sediments such as their origin in addition to the
39 common measurements of concentrations and discharge rates. Some rapid and low-cost fingerprinting
40 methods based on spectroscopy have recently been developed. We investigated how visible spectra
41 could be used to predict the proportion of source material in suspended sediment samples, paying
42 particular attention to the potential alteration of the spectrophotometric signatures between soils and
43 suspended sediments during transport.

44 *Materials and methods* The 22-km² catchment studied was composed of black marls, limestones,
45 molasses, undifferentiated deposits and gypsum. Forty-eight source materials were sampled and 328
46 suspended sediment samples were collected at the outlet during 23 runoff events. Measurements were
47 taken with a diffuse reflectance spectrophotometer on dried samples. As the erosion processes are
48 particle size selective, five size fractions of source material were measured in order to assess the
49 potential alteration of the signatures. As the biogeochemical processes occurring in the river could
50 also affect the signatures, source materials having been immersed in the river for durations ranging
51 from 1 to 63 days were measured. Finally, partial least-squares regression models were constructed on
52 81 artificial laboratory mixtures to predict the proportion of source material.

53 *Results and discussion* The spectrophotometric measurements discriminated the primary source
54 materials but not the Quaternary deposits. As the gypsum was not conservative, only the black marls,
55 molasses and limestones were used in the fingerprinting procedure. The construction of the partial
56 least-squares regression models led to a median absolute error of 1.1%. This error increased to 3.9%
57 when the models were applied to source samples with i) different particle sizes, ii) different durations
58 spent in the river or iii) different origins than those used for their construction. The effect of particle
59 size on the fingerprinting procedure was larger than the effect of biogeochemical reactions or the
60 spatial variability of the spectrophotometric signatures. Half of the 23 runoff events analysed
61 exhibited huge variations in the source proportions from one collected sample to another.

62 *Conclusions* The spectrophotometric fingerprinting approach proved its ability to quantify routinely
63 the proportion of primary source materials in all suspended sediment samples collected during runoff
64 events using automatic sequential samplers. The high temporal resolution of the predicted proportions
65 revealed that, analysing three or four suspended sediment samples only during a runoff event would
66 lead to a complete misunderstanding of the hydro-sedimentary processes for more than half of the
67 investigated runoff events.

68
69 **Keywords** Conservative tracer properties • Diffuse reflectance spectrometry • Fingerprinting •
70 Mountainous catchment • Partial least-squares regression • Suspended sediments • Visible range

71

72 **1 Introduction**

73 Given the importance and the recurrence of economic and environmental problems due to erosion and
74 fine sediment transport (Pimentel et al. 1995; Owens et al. 2005; Boardman 2006; Almansa et al.
75 2012), decision makers' demands for efficient on- and off-site mitigation measures to limit exports of
76 suspended sediments are becoming more insistent. Physically based distributed models are required to
77 assess these mitigations in a context of changes in meteorological forcing and soil use. However, it is
78 clear that at present, the performance of these models remains poor and far below the predictive
79 expectations of decision makers (Mitas and Mitasova 1998; Nearing 1998; Jetten et al. 1999, 2003;
80 Evans and Brazier 2005; Beven 2006, Boardman 2006). This may be due to a large extent to the fact
81 that these models focus only on what occurs at the catchment outlet (Jetten et al. 1999) and to the
82 associated strong likelihood of predicting the correct results for the wrong reasons (Favis-Mortlock et
83 al. 1996; Jetten et al. 1996; Takken et al. 1999). Behind this well-known problem, additional issues
84 associated with the spatial and temporal dynamics of processes occurring within catchments still
85 exist. Among them, the spatio-temporal patterns of rainfall (Soler et al. 2007; Nadal-Romero et al.
86 2008; Mano et al. 2009; Navratil et al. 2012) and the strong spatial heterogeneity of soil erodibility is
87 crucial (Gallart et al. 2002; Gumiere et al. 2011; Wang et al. 2009; López-Tarazón et al. 2010). In this
88 context, gaining knowledge on the variability of sediment sources during runoff events should
89 provide important insights to better understand the hydro-sedimentary dynamics at the catchment
90 scale (Collins and Walling 2004; Walling 2005). Moreover, the extremely high temporal variability of
91 suspended sediment fluxes that can occur in many environments, as reported for instance by Duvert et
92 al. (2010) and Evrard et al. (2010) in mountainous catchments, suggests that suspended sediment
93 sources transiting at outlets may also exhibit strong variations during runoff events. This emphasizes
94 the need to characterize the suspended sediment source routinely on all samples collected during
95 runoff events using automatic sequential samplers. However, conventional fingerprinting techniques
96 based on geochemical and radionuclide measurements that have been used over the last 30 years
97 (Walling 2005; Davis and Fox 2009) are time-consuming and rather expensive (Martínez-Carreras et
98 al. 2010b; Poulénard et al. 2012), which may prevent routine characterization of large numbers of
99 samples representative of various sediment sources and hydrodynamic conditions.

100 Because spectroscopy is a rather rapid, inexpensive, non-destructive and straightforward technique, it
101 has been commonly used during the past 10 years in the visible (VIS), near infrared (NIR) and mid-
102 infrared (MIR) ranges in order to quantify soil properties (Viscarra Rossel et al. 2006). More recently,
103 spectroscopy has been applied to suspended sediment source tracing and has proved its ability to
104 discriminate and quantify various source materials in suspended sediment samples (Poulénard et al.
105 2009; Martínez-Carreras et al. 2010a and b). So far, spectral reflectance data have been used in three
106 different ways. Colour coefficients deduced from VIS spectra were used directly in an optimised
107 mixing model as potential fingerprint properties (Martínez-Carreras et al. 2010a). VIS/NIR spectra
108 were also used to predict the concentrations of specific geochemical fingerprints which were then used

109 in an optimised mixing model (Martínez-Carreras et al. 2010b). The last approach consisted in directly
110 using NIR/MIR spectra to estimate the proportion of the different source materials in suspended
111 sediment samples after conducting a partial least-squares regression calibration on artificial source
112 material mixtures (Poulenard et al. 2012). However, so far and to our knowledge, there has not been
113 any attempt to use VIS spectra and deduced colorimetric parameters as potential predictors of the
114 proportion of the different source materials in suspended sediment samples according to the previously
115 described approach.

116 Even though the measurement of VIS spectra is recognised as being a good predictor of soil
117 constituents (Debret et al. 2011) and a simple methodology, even faster and cheaper than for infrared
118 methods, some assumptions must be verified before using them as potential tracers in the framework
119 of a fingerprinting study. Tracing a suspended sediment source based on soil measurements and
120 suspended sediment at the catchment outlet assumes that the source soil signatures are preserved
121 (Foster and Walling 1994). However, two major processes occurring during soil erosion and sediment
122 transport at the catchment scale could affect these signatures. Firstly, erosion processes are known to
123 be size selective (Slattery and Burt 1997; Malam Issa et al. 2006). Given that grain size is a physical
124 chromophore (Ben-Dor et al. 1998), the signatures measured downstream on suspended sediment may
125 differ from the source soils. Secondly, biogeochemical reactions such as iron reduction (Philips and
126 Marion 2001) can occur during the transport of source soil particles leading to differences in
127 spectroradiometric signatures.

128 The objectives of this study were i) to assess whether spectroradiometric signatures were preserved
129 between source soil material on hillslopes and suspended material collected at the catchment outlet, ii)
130 to quantify the fractions and associated uncertainty of each potential source material in suspended
131 sediment samples during runoff events and iii) to assess the range of the suspended sediment source
132 variations during runoff events at the outlet of a mountainous catchment.

133

134 **2 Materials and methods**

135 2.1 Catchment characteristics and source soil sampling

136 The 22-km² Galabre catchment is part of a larger mountainous instrumented area in the southern
137 French Alps (Fig. 1a). It is located in a sedimentary area characterised by five main source material
138 (see Fig. 1b), i.e. black marls (9%), limestones (54%), molasses (4%), undifferentiated deposits (29%)
139 and gypsum (4%). The soils are shallow with maximum depths of 60 cm. The catchment is well
140 covered by vegetation (forest and grassland), cropland accounting for only 2% of the total area.
141 However, 8% of its area is considered as highly erodible. These highly erodible areas were defined as
142 zones without vegetation and characterised by the presence of erosion features such as rills, gullies or
143 badland morphology (Navratil et al. 2012). They were delineated in a GIS using 2004 aerial
144 photographs and validated by field observations. These areas are assumed to be the major contributors
145 to the suspended sediment loads since they are well connected to the hydrographic network. We

146 should also stress that these areas, which are considered as potential sediment sources, cannot be
147 considered as soils because soil horizons cannot be distinguished; the materials are much more similar
148 to the original geological material (Fig. 1b).

149 In September 2008, a sampling campaign was conducted. Forty-eight samples were collected of the
150 top 5 cm of each material following a stratified sampling approach. The stratification consisted of
151 dividing eroded areas into five homogeneous subgroups based on their lithology prior to the field
152 campaign. Samples were then collected in eroded areas corresponding to each subgroup, depending
153 on terrain access facility (see Fig. 1b).

154

155 **2.2 Catchment outlet and monitoring station**

156 The outlet of the Galabre catchment (lat.: 44°10'28"N, long.: 06°13'07"E) was equipped in spring
157 2007 to monitor suspended sediment dynamics. The water level was measured by a 24-GHz radar
158 (Paratronic Crusoe®) every 10 min. The water-level discharge rating curve was built based on ~40
159 salt gauging measurements. Turbidity was measured every 10 min by infra-red light retro-diffusion
160 (nephelometric turbidimeter WTW Visolid® 700-IQ). The turbidimeter was calibrated by using
161 measurements of suspended sediment concentration of river water samples collected automatically
162 (Teledyne ISCO® 176 3700) every 60 and 30 min when turbidity critical thresholds were exceeded,
163 i.e. $t_1=5 \text{ g L}^{-1} \text{ SiO}_2$ and $t_2= 20 \text{ g L}^{-1} \text{ SiO}_2$, respectively. The suspended sediment concentration was
164 measured by weighing the sample after drying it for 24 h at 105°C. More information on this gauging
165 station and the associated uncertainties is provided in Navratil et al. (2011). The mean discharge was
166 $0.256 \text{ m}^3 \text{ s}^{-1}$ over the 2007–2011 recording period, with a maximum discharge of $34 \text{ m}^3 \text{ s}^{-1}$. The mean
167 suspended sediment concentration was 0.4 g L^{-1} with a maximum value of 217 g L^{-1} . The mean area-
168 specific suspended sediment yield was $651 \text{ t km}^{-2} \text{ y}^{-1}$.

169

170 **2.3 Spectrocolorimetric measurements**

171 Spectrocolorimetric measurements were taken on both suspended sediment samples collected during
172 runoff events ($n = 328$) and on source soil materials ($n = 48$). It should be noted that the fingerprinting
173 technique presented in this paper was designed to be further applied routinely on each collected
174 suspended sediment sample once it had been dried at 105°C and weighed to obtain the suspended
175 sediment concentration. In order to avoid a bias between suspended sediment samples and source
176 material samples, all of them were dried at 105°C for 24 h and stored in 60 mL polystyrene straight
177 containers before taking measurements.

178 Measurements were taken using a portable diffuse reflectance spectrophotometer (Konica Minolta
179 2600d) integrating its measurement on a 3-mm radius circle. The spectrophotometer was installed
180 upside-down, face up, and the tubes containing the samples were placed on the measuring cell. Thus
181 the measurement was taken directly through the base of the tube. The minimum amount of sample
182 was roughly 100 mg. Because of the rather small measuring area and to account for the possible

183 heterogeneity within the samples, four measurements were taken on each sample, the container being
184 shaken between each measurement. During a measurement, the spectrophotometer emits a standard
185 Xenon arc light source and measures the ratio between the light reflected from the sample and from a
186 calibrated white standard. Spectral reflectances were measured between 360 and 740 nm with a 10-
187 nm resolution. All measurements were taken with the D65 standard illuminant, the 10° angle observer
188 and with the specular component excluded. Raw data collected were the spectral reflectance
189 percentage for each of the 39-wavelength class. From these raw data we also derived 8 components of
190 various colorimetry models (Viscara Rossel et al. 2006). XYZ tristimulus values were calculated
191 based on the colour-matching functions defined in 1931 by the International Commission on
192 Illumination (CIE, 1931). We then transformed the standardised tristimuli to the CIE L*a*b* and the
193 CIE L*u*v* cartesian coordinate systems using the equations given in CIE (1978).
194 The spectrophotometer was calibrated before each set of measurements by making a zero and a white
195 calibration. Control measurements were also taken regularly during and at the end of a set of
196 measurements. These latter consisted in measurements on red, green and yellow panels as well as six
197 contrasted soil samples.

198

199 **2.4 Assessment of the conservation of the colour-based signatures**

200 *2.4.1 Particle size measurements and fractioning*

201 Particle size distributions were measured using a laser diffraction sizer (Malvern, Mastersizer 2000)
202 in the 0.01- to 2000- μm range. As the objective of these measurements was to identify the particle
203 size selectivity during erosion processes, absolute particle size distribution rather than the effective
204 particle size distribution were measured on the <63- μm size fraction on a selection of 17 soil samples
205 and 47 suspended sediment samples. Particle size distributions measured after 10 min of sonication
206 with maximum stirring and pumping conditions, at 1000 and 2500 rpm, respectively, were considered
207 as absolute particle size distributions.

208 Source soils were fractioned in order to assess to what extent the size of particles was responsible for
209 the colour-based signatures. For each source material, black marls, limestones and molasses, five
210 source soil samples were sieved to five size fractions: bulk soil, <200, <100, <63 and <20 μm .

211

212 *2.4.2 In situ biogeochemical experiment*

213 To assess a possible alteration of the colour-based signatures during the transit of suspended
214 sediment, source soil samples were immersed for various durations in the Galabre River. The
215 experiment was conducted on the <63- μm size fraction of the potential source materials. The samples
216 were composite samples consisting of a mix of three to five individual samples from the same
217 lithology. For each composite source material, 2 g of soil were introduced in two successive nylon
218 porous bags with a 20- μm mesh size. Preliminary trials revealed that both the mesh size and the
219 double layer provided a good compromise for the renewal of water in the bags without clogging by

220 external suspended sediment with limited initial material loss. Indeed the comparison of the mass
221 before and after immersion led to a low median mass loss of 5% (statistically significant according to
222 a Wilcoxon signed ranked test). A similar comparison for the D10, D50 and D90 on the dispersed
223 particle size distributions did not reveal the existence of any significant difference. Forty-five bags
224 were immersed in the river in March 2009. Then three triplicates of each source material were
225 collected after 1, 7, 14, 35 and 63 days. Spectral properties were measured on each sample collected,
226 once oven dried for 24 h at 105°. We emphasize that this experiment was conducted with immersion
227 durations more than four times longer than those reported in Poulenard et al. (2012) with the same
228 source materials.

229

230 *2.4.3 Statistical tests*

231 To assess whether groups of measurements were significantly different, statistical tests of group
232 comparisons were done. As the groups compared did not exhibit equality in their variance, the Dunn
233 nonparametric test was used at the 0.01 probability level. This test was applied to address three goals.
234 It was used to assess the extent to which particle size selectivity occurred during sediment transfer. For
235 each dispersed size fraction, a comparison was made between suspended sediment and source
236 materials. The Dunn test was also applied to assess potential changes in source soil signatures i)
237 between various particle size fractions and ii) between various duration times spent in the river. Each
238 colorimetric parameter value group was compared to the group measured on the <63- μ m size fraction
239 and to the group measured after 1 day in the river, respectively for i) and ii). These comparisons were
240 done for each parameter L^* , a^* , b^* , u^* , v^* and for each source material.

241

242 **2.5 Construction of predictive models**

243 Partial least-squares regression models were constructed following the methodology presented by
244 Poulenard et al. (2012) to quantify the proportion of each source material in the suspended sediment
245 samples collected during runoff events. Partial least-squares regression models were constructed by
246 establishing relationships between spectral measurements together with derived colorimetric
247 parameters (47 X-explanatory variables) and proportions of source materials in various samples (Y-
248 variable), as described by Wold et al. (2001). At the end of the discriminant analysis of source
249 materials by spectrophotometry (section 3.1.), only three primary source materials were retained for
250 the construction of the partial least-squares regression models (i.e., black marls, limestones and
251 molasses). Thus, 81 artificial laboratory mixture samples were prepared by mixing, in known
252 proportions, these three primary source materials that were immersed for 1 day (Fig. 2). The
253 distribution of the mixtures in the ternary diagram was a compromise between covering the whole
254 triangle area and having a number of samples that were well distributed on each axis. As the spectral
255 measurements were repeated four times on each sample, the number of samples used for the partial
256 least-squares regressions reached 324. This data set was randomly divided, one half being used for

257 calibration, the remaining half for validation. Independent partial least-squares regression models
258 were constructed for each primary source material type. Finally, the quality of the tracing procedure
259 was then checked by summing the three predicted proportions and verifying that this sum was close to
260 100%.

261

262 **3 Results and discussion**

263 **3.1 Source soil discrimination**

264 The first step of the proposed tracing approach was to assess whether the spectrophotometric
265 measurements were able to discriminate the various source materials in the Galabre catchment. The
266 factorial discriminant analysis performed on the values of each colorimetric parameter for the 48
267 source material samples revealed that spectrophotometry provided a way to distinguish all groups of
268 samples. The cumulative percentage of discrimination of the first two factors was 100%. The
269 parameter a^* exhibited a correlation of 0.99 with the first factor while L^* exhibited a correlation of
270 0.95 with the second factor. As illustrated by Fig. 3 showing the scattering of L^* and a^* parameters,
271 78% of the samples were grouped in four sets. Samples with L^* values comprised between 33.3 and
272 38.3 and a^* values between 1.5 and 1.9 corresponded to black marls. Molasses were clearly
273 discriminated from black marls by L^* values ranging from 53.3 to 56.5 and a^* values ranging from
274 0.7 to 1.1. Limestones were fully discriminated from the two previous source material types by higher
275 a^* values ranging from 9.2 to 10.1. The fourth group, gypsisols, was also well discriminated from the
276 other source materials with the highest L^* values ranging from 66.8 to 71.7. The remaining 22% were
277 samples covering the entire range of L^* and a^* variations without showing any direct affiliation to
278 one of the four previous groups. The latter samples appeared to comprise a mix of the other source
279 materials. This was expected because these samples were sampled on steep slopes in areas labelled as
280 undifferentiated deposits. The classification table (i.e. confusion table) used to appraise the results of
281 the predictive quadratic discriminant analysis confirmed that black marls, molasses, limestones and
282 gypsisols were accurately classified (100% correct), whereas undifferentiated deposits were classified
283 with a lower accuracy (73% correct). As no proper colorimetric signature was found for these
284 materials that are a mix of the four others, they were no longer considered as a primary source
285 material in the subsequent tracing approach based on spectrophotometric measurements. Among the
286 four remaining potential source materials, the gypsisols showed by far the least conservative
287 behaviour during their transfer by the flow. Indeed gypsum is known to be highly soluble in water
288 (Porta 1998) and the Diffuse Reflectance Infrared Fourier Transform Spectrometry measurements
289 taken by Poulenard et al. (2012) revealed the absence of gypsum in suspended sediment samples
290 collected at the outlet of the Galabre catchment. Thus the gypsisol potential source material was
291 removed from the subsequent steps of the tracing approach.

292

293 3.2 Effect of particle size on source signature

294 The particle size selectivity of erosion and transport processes occurring in the Galabre catchment
295 was assessed by comparing the dispersed particle size distributions measured on 17 of the 48 source
296 material samples and on 47 of the 328 suspended sediment samples. Figure 4a shows evidence that
297 the <63- μm size fraction of the suspended sediment samples was enriched in particles smaller than 8
298 μm and depleted in particles coarser than 16 μm . In order to assess down to which size fraction the
299 erosion and transport processes were size selective, we calculated the class weights considering first
300 the <31- μm size fraction only (see Fig. 4b) and then the <16- μm size fraction only (see Fig. 4c).
301 Figure 4b shows that, even when focusing on the <31- μm size fraction, the suspended sediment
302 samples were still depleted in the coarsest size fractions. However, when considering the <16- μm size
303 fraction only, no statistical difference according to the Dunn test was observed between the suspended
304 sediment and the source materials (see Fig. 4c). This analysis did not allow for a precise identification
305 of the critical size, below which particle size selectivity no longer existed. It is likely that this size
306 limit was located somewhere in the 16- to 31- μm range for the runoff events studied and in the
307 Galabre mountainous catchment. Nevertheless, it underlined the need for considering particle size
308 selectivity in fingerprinting approaches far below 63 μm and certainly down to particle size around
309 roughly 20 μm . In the following, we investigated the extent to which the spectrophotometric
310 signatures varied between the various particle size fractions.

311 Figure 5 shows the same trend for all the colorimetric parameters and the source materials.
312 Considering the three source materials, the average increase of the colorimetric values from the bulk
313 samples to the <20- μm size fraction were 11%, 40%, 23%, 28% and 24%, respectively, for L^* , a^* ,
314 b^* , u^* and v^* . These changes were quite high and remained in agreement with already published data
315 on the colour-particle size relationship (Torrent and Barron, 1993; Sánchez-Marañón et al., 1997;
316 Sánchez-Marañón et al., 2004; Gunal et al., 2008). However, these changes fall to 6%, 5%, 6%, 7%
317 and 7%, respectively, for L^* , a^* , b^* , u^* and v^* when comparing the <63- μm size fraction to the <20-
318 μm size fraction. As no significant statistical difference was found between the two latter fractions
319 according to the Dunn test (see Fig. 5), we assumed that constructing the partial least-squares
320 regression models on the <63- μm size fraction should lead to representative predicted proportions of
321 source materials in the suspended sediment samples. Nevertheless, the changes observed on the
322 colorimetric parameters certainly generated uncertainty in the predicted source proportions (see
323 section 4.4). It should be noted that some particles reaching 300 μm in size were sometimes sampled
324 during runoff events. However, for the 47 suspended sediment samples in which we analysed particle
325 size distribution, the >63- μm size fraction accounted for an average of only 1.1% of the entire sample
326 particle size distribution. Thus, even though the change in colorimetric parameters associated with
327 coarse particles was high, this effect can generally be ignored when comparing the <63- μm size
328 fraction to the <200- μm size with values of -5%, -16%, -11%, -13%, -11%, respectively, for L^* ,
329 a^* , b^* , u^* and v^* .

330
331
332
333
334
335
336
337
338
339
340
341
342
343
344
345
346
347
348
349
350
351
352
353
354
355
356
357
358
359
360
361
362
363
364

3.3 Effect of immersion duration on source signature

Colorimetric parameters L^* , a^* , b^* , u^* and v^* generally exhibited low variations according to the immersion time of source samples in the river (Fig. 6). Indeed, the variations that affected the original source material (day 0) remained lower than 10% for the whole set of parameters, source materials and immersion durations. This means that no major differences were observed i) between measurements taken on original source materials (day 0) and measurements taken on the materials having been immersed in the river and ii) between the various measurements taken for increasing immersion durations.

However, looking at the small variations in detail highlighted differences between source materials. For each parameter, the relative differences between $t = 1$ day and the subsequent durations were calculated. Throughout all immersion durations, the differences were found to be lower than 2.6% on average for the limestone samples, whereas they were higher for the molasses and black marls. For example, the black marls exhibited average differences of 6.3, 3.8, 7.3, 5.5 and 6.6%, respectively, for the L^* , a^* , b^* , u^* and v^* parameters. The greater differences observed for molasses and black marls than for limestones were also confirmed by statistical tests of group comparisons shown in Fig. 6 as gray circles. Doing the same analysis but over all the parameters for each immersion duration led to small average differences (i.e. less than 3.2%) for limestones. No clear trend was noted with increasing residence time in the river flow. Larger differences were obtained, however, for the molasse and the black marl samples. The largest differences were obtained for the last two immersion durations (days 35 and 63) with average values of 7.2 and 9.8% for the molasses and black marls, respectively. This trend was also confirmed by statistical tests, as shown in Fig. 6.

Overall, this detailed analysis showed that the black marls and molasses may be more sensitive to colorimetric variations during their transit times than the limestone material. It also underlined that, for the two most sensitive materials, the longest periods (i.e. longer than 1 month) in the river were associated with the largest variations of the spectrophotometric signatures. This result complements similar work conducted by Poulenard et al. (2009, 2012) on the effect of short immersion durations of less than 1 month on infrared spectra. Whatever spectral range is used, this highlights the need for further investigation with longer times spent in the river, as the transfer time distribution of suspended sediments within rivers could be longer than the 65-day duration tested in this study, as demonstrated by Bonniwell et al. (1999) and Evrard et al. (2010) in mountainous headwater catchments. Even if the variations of the colorimetric parameter values with the time spent in the river water were rather small for our experimental conditions, the impact of this associated signature alteration on the final fingerprinting procedure will be discussed in the following section.

365 **3.4 Colour-based mixing models**

366 Figure 7 shows the performance of the three partial least-squares regression models constructed
367 independently for the three source materials. The determination coefficients were similar for each
368 model (0.99), whereas the root mean square errors were slightly different with values of 1.83, 2.28
369 and 1.55, for black marls, molasses and limestones, respectively. Considering the whole data set used
370 in the construction of the partial least-squares regression models (i.e. training and validation) led to a
371 median sum of the three predicted source proportions of 100.0% with minimum sums of 97.7% and
372 maximum sums of 103.3%. These rather good results for the sums were only representative of the
373 laboratory mixtures made with the three source soil materials sieved to 63 μm and immersed in the
374 flow for 1 day. We then assessed the performance of these partial least-squares regression models
375 when predicting proportions of source samples with different particle size distribution or different
376 immersion durations than those used to construct the models. As mentioned by Martínez-Carreras et
377 al. (2010a and 2010b) and by Poulénard et al. (2012), error could also propagate in the models
378 because of the spatial variability of the source material signature. Even if the variability of the
379 colorimetric parameters within a group of source material samples was rather low (see Fig. 3), we
380 assessed the errors generated by this spatial variability.

381 The overall absolute errors were larger, with values of 3.9%, 1.6% and 8.4%, respectively, for the
382 median, the first quartile and the third quartile, whereas these values reached only 1.1%, 0.5% and
383 2.1% for the training and validation data set used during the construction of the partial least-squares
384 regression models. Errors for the samples that were immersed for different durations
385 in the river (Table 1) were rather small with a median value of 3.1%. Whilst these latter allowed to
386 isolate the errors associated with the alteration of the signatures due to immersion, errors in Table 2
387 included not only the effect of particle size, but also the effect of the spatial variability of the source
388 material samples within a single group of source material. The measurements were indeed conducted
389 on individual samples, whereas the models were calibrated on composite samples sieved to 63 μm .
390 Thus the median error of 3.3% corresponding to the <63- μm size fraction reflects the effect of spatial
391 heterogeneity of the source materials. It was however not possible to precisely isolate the effect of the
392 size fractions. It should be noted that the median error increased to 11.5% when considering the other
393 size fractions (Table 2). This suggests that the effect of particle size selectivity on the
394 spectroradiometric fingerprinting procedure was larger than the effect of spatial heterogeneity or
395 biogeochemical reactions that may have occurred during the particle transit times. The 3rd quartile
396 errors, which was considered to be more realistic than the median error to account for the range of
397 uncertainty, was below 20% for the smallest size fractions, i.e. <63 μm and <20 μm (see Table 2). As
398 on average 98.9% of the suspended sediment samples were smaller than 63 μm , the overall maximum
399 error could reasonably be considered smaller than 20% when applying this spectroradiometric
400 fingerprinting procedure to predict the proportion of a source material in suspended sediment sampled
401 during runoff events. However, this uncertainty was only valid in the range of conditions tested in this

402 study. The uncertainty would be larger if i) suspended sediments had transit times longer than 63
403 days, ii) particle sizes were finer than 20 μm or larger than 63 μm and iii) suspended sediments came
404 from non-sampled source materials.

405 As reported previously, calculating the sum of the predicted proportions for the three material sources
406 obtained with the three independent partial least-squares regression models provided a way to control
407 the reliability of the predictions. As the gypsum source material was not retained in the colour-based
408 fingerprinting procedure, we assessed whether the latter control procedure was able to identify that a
409 problem occurred when we conducted our fingerprinting approach on the samples. Therefore VIS
410 measurements were conducted on the <63- μm fraction of 20 gypsum source material samples as if
411 they were suspended sediments sampled during runoff events. The three partial least-squares
412 regression models were then applied to the measurement data sets in order to obtain predicted
413 proportions of black marls, molasses and limestones. The sum of the three predicted proportions was
414 on average 145% with maximum values of 180%, suggesting that the control procedure could detect
415 problems during the fingerprinting approach. This control procedure should be considered as a
416 necessary but not a sufficient condition to confirm the reliability of the method. When the sum is very
417 different from 100%, as for the gypsum samples, there is definitely a problem with the model.
418 However the sum might be close to 100% and there will be no guarantee that the model is correct.

419

420 **3.5 Prediction of source material proportion in suspended sediment samples collected during** 421 **runoff events**

422

423 The uncertainty associated with the spectrophotometric fingerprinting procedure could be considered
424 as rather high, in comparison with errors reported by the conventional fingerprinting approach studies
425 based on geochemistry and radionuclide properties (Collins et al. 2012). However, one may wonder if
426 these errors are acceptable given the range of variations in the proportions of sources during a runoff
427 event. In order to assess how much the suspended sediment source varied during runoff events at the
428 Galabre river outlet, we applied the partial least-squares regression models to predict the proportions
429 of black marls, limestones and molasses during 23 runoff events recorded and sampled between
430 November 2007 and November 2011. On average, for the 328 suspended sediment samples collected
431 and analysed, the sum of the three predictions reached 106%. For 18 out of the 23 runoff events
432 analysed, the corresponding sums remained below 120% for all the intra-event suspended sediment
433 samples (Fig. 8). For four of the five remaining runoff events, only one or two suspended sediment
434 samples were characterised by unusually high sum values (maximum, 141%). However, almost half
435 (11) of 23 suspended sediment samples collected during the remaining 07/07/10 runoff event were
436 characterised by predicted black marl proportions larger than 120% (see Fig. 8).

437 For the 23 runoff events, the predicted limestone proportions remained small (10% on average),
438 which should be considered as negligible regarding the estimated uncertainty associated with the

439 colour-based fingerprinting procedure. Only 18 suspended sediment samples exhibited predicted
440 limestone proportions higher than 20%. The suspended sediment samples were therefore mostly
441 composed of black marls and molasses, both exhibiting concomitant variations in their proportions, as
442 illustrated by the numbers in figure 8 showing their temporal evolution during the 08/11/11 runoff
443 event. In order to assess the value of applying spectrophotometric tracing to the maximum of samples
444 within runoff events, we calculated the variation of each predicted black marl proportion from one
445 sample to the next collected automatically during a runoff event. We restricted this analysis to black
446 marls because they exhibited concomitant variations in their proportions with molasses. The runoff
447 events were then classified into three different groups based on an a priori criteria, i.e. the number of
448 samples within an event characterised by variations higher than 50% (Table 3). Events from the first
449 group had predicted proportions smaller than 10%, i.e. remaining stable throughout the runoff event.
450 Events from the second group had only one sample with variations higher than 50%. The highest
451 variations were observed in the early moments of runoff events, decreasing rapidly to values smaller
452 than 25%. Events from the third group were characterised by highly variable predicted proportions
453 from one sample to another. More than half of the 23 runoff events were considered as highly
454 variable. Even though the first two groups of runoff events could be well characterised in terms of
455 source material dynamics by analysing no more than three or four suspended sediment samples during
456 an event, applying the same strategy for runoff events of the last group would lead to a complete
457 misunderstanding of the hydro-sedimentary processes.

458 For two of the 23 runoff events (22/11/07 and 12/08/08), proportions of sources determined by two
459 other tracing methods were available, i.e. the method combining diffuse reflectance infrared Fourier
460 transform spectrometry with partial least-squares regression (Poulenard et al. 2012) and a more
461 conventional geochemical fingerprinting method (Navratil et al. 2012). Figure 9 shows a general good
462 agreement between the methods if the uncertainty associated with the predicted black marl
463 proportions is considered. The differences between the different fingerprinting techniques may be
464 largely due to i) the ability of each method to consider the variability of the source materials'
465 fingerprinting properties from the step of selecting the most discriminating tracers to the predictive
466 model construction step, ii) the potential alteration of the selected fingerprinting properties during the
467 transit of particles in the watershed, recognising that different techniques are more or less sensitive to
468 these alterations depending on the properties selected.

469 To conclude with the potentiality of the spectrophotometric fingerprinting procedure, it is clear that
470 two main limitations remain in comparison with conventional fingerprinting methods. The first one is
471 the lack of discrimination compared to sources other than the primary source materials, such as the
472 undifferentiated deposits in this catchment. As mentioned by Martínez-Carreras et al. (2010c), this
473 lack of discrimination may also be a limitation for larger catchments characterised by a greater
474 variability in the colorimetric signatures. This issue should be further investigated, for example by
475 combining the method presented in this study with conventional fingerprinting methods. The second

476 limitation is the rather high errors on the predicted proportions of source materials. Even if these
477 limitations exist, the main advantages of the procedure (i.e., low cost and rapidity) facilitate the
478 achievement of numerous measurements and hence high-resolution predictions of proportions of
479 primary source materials in suspended sediment samples, which is essential for better understanding
480 the behaviour of headwater catchments exhibiting highly variable hydro-sedimentary dynamics.

481

482 **4 Conclusions**

483 The colour-based fingerprinting approach conducted in a 22-km² mountainous catchment
484 demonstrated that four of the five main source type materials, i.e. black marls, limestones, molasses
485 and gypsisols, could be discriminated by means of spectral measurements conducted in the visible
486 range. However, it was not possible to fingerprint the undifferentiated deposits, composed of a mix of
487 the four other source materials in various proportions. This should be considered as the technique's
488 main limitation. The colour-based fingerprinting approach was found to be able to discriminate the
489 primary source materials.

490 As the suspended sediment samples were enriched in particle sizes finer than (roughly) 20 µm in
491 comparison with source materials, which is rather small for a rapidly flowing river, the
492 conservativeness of the colour-based signatures was challenged. Another debated issue was the
493 potential alteration of spectrophotometric signatures during the transit of the suspended sediments in
494 the hydrographic network, as suspended sediment transit times within the river channel can be larger
495 than the concentration time of the catchment. The experiments designed to answer these two
496 questions revealed that the effect of particle size on the colour signature was higher than the effect of
497 the duration of sediment immersion in the river water. A maximum 16% variation of the colorimetric
498 parameters was measured between the <63 µm fractions and the other size fractions observed during
499 runoff events, whereas a maximum variation of 10% was measured in the samples having been
500 immersed between 1 and 63 days. Nevertheless, these rather high variations did not generate
501 excessive uncertainty through the partial least-squares regression mixing the calibration and
502 prediction procedure, because an error of 20% should reasonably be associated with the predicted
503 proportions of source materials in suspended sediment samples. Such uncertainty remained much
504 higher than the uncertainty associated with the conventional fingerprinting approach and could
505 certainly be reduced. Since the effect of particle size was found to be significant, we could for
506 instance have considered applying correction factors, as is done in mixture models of conventional
507 fingerprinting approaches. This would mean routinely measuring the particle size distributions, which
508 is time-consuming, and could reduce one of the main advantages of this alternative method, i.e.
509 analytical rapidity.

510 Finally, the application of the partial least-squares regression models to 23 runoff events revealed that
511 the predicted proportions of black marls and molasses were highly variable within runoff events that
512 occurred in the Galabre catchment from November 2007 to November 2011. The data set produced

513 with this colour-based fingerprinting approach on a significant number of runoff events, each being
514 well documented, should now be analysed considering the positioning of the source materials in the
515 catchment, the spatiotemporal meteorological radar data, the time series of discharges and
516 concentrations at the outlet. This should offer new insights into the hydrosedimentary processes and
517 assessing the performance of distributed hydrological models.

518

519 **Acknowledgements** This work was funded by the French National Research Agency
520 (ANR/BLAN06-1_139157) and the National Center of Scientific Research (INSU/EC2CO-CYTRIX
521 2011). The authors wish to thank all the members of the project for fruitful discussions and for many
522 helpful comments. They also thank Julieta Bramorski, Amélie Douchin and Antoine Chiaverini for
523 their help during their training periods.

524

525 **References**

- 526 Almansa C, Calatrava J, Martinez-Paz JM (2012) Extending the framework of the economic
527 evaluation of erosion control actions in Mediterranean basins. *Land Use Policy* 29: 294-308
- 528 Ben-Dor E, Irons JR, Epema GF (1998) Soil reflectance. In: Rencz AN (ed) *Remote sensing for the*
529 *earth sciences. Manual of remote sensing.* John Wiley & Sons, New York, pp 111-188
- 530 Beven K (1989) Changing ideas in hydrology. The case of physically based models. *J Hydrol* 105(1–
531 2):157-172
- 532 Beven K (2006) On undermining the science? *Hydrol Proces* 20:2050-2065
- 533 Bonniwell EC, Matisoff G, Whiting PJ (1999) Determining the times and distances of particle transit
534 in a mountain stream using fallout radionuclides. *Geomorphology* 27:75-92
- 535 Boardman J (2006) Soil erosion science: reflections on the limitations of current approaches. *Catena*
536 68:73-86
- 537 Collins AL, Walling DE (2004) Documenting catchment suspended sediment sources: Problems,
538 approaches and prospects. *Prog Phys Geog* 28:159-196
- 539 Collins AL, Zhang Y, McChesney D, Walling DE, Haley SM, Smith P (2012) Sediment source tracing
540 in a lowland agricultural catchment in southern England using a modified procedure combined
541 statistical analysis and numerical modelling. *Sci Total Environ* 414:301-317
- 542 Commission Internationale de l'Eclairage (CIE) (1931) *CIE Proceedings*, Cambridge University Press,
543 Cambridge, UK
- 544 Commission Internationale de l'Eclairage (CIE) (1978) *Recommendations on Uniform Color Spaces,*
545 *Color Differences, and Psychometric Color Terms.* Colorimetry CIE, Paris Suppl. no. 2 to
546 Publication no. 15
- 547 Davis MD, Fox JF (2009) Sediment fingerprinting: review of the method and future improvements for
548 allocating non point source pollution. *J Environ Eng* 135:490-504

549 Debret M, Sebag D, Desmet M, Balsam W, Copard Y, Mourier B, Susperregui AS, Arnaud F,
550 Bentaleb I, Chapron E, Lalier Verges E, Winiarski T (2011) Spectrocolorimetric interpretation of
551 sedimentary dynamics : the new “Q7/4 diagram”. *Earth Sci Rev* 109:1-19

552 Duvert C, Gratiot N, Evrard O, Navratil O, Némery J, Prat C, Esteves M (2010) Drivers of erosion and
553 suspended sediment transport in three headwater catchments of the Mexican Central Highlands.
554 *Geomorphology* 123:243-246

555 Evans R, Brazier R (2005) Evaluation of modelled spatially distributed predictions of soil erosion by
556 water versus field-based assessments. *Environ Sci Policy* 8:493-501

557 Evrard O, Némery J, Gratiot N, Duvert C, Ayrault S, Lefèvre I, Poulenard J, Prat C, Bonté P, Esteves
558 M (2010) Sediment dynamics during the rainy season in tropical highland catchments of central
559 Mexico using fallout radionuclides. *Geomorphology* 124:42-54

560 Favis-Mortlock DT, Quinton JN, Dickinson WT (1996) The GCTE validation of soil erosion models
561 for global change studies. *J Soil Water Conserv* 51(5):397-403

562 Foster IDL, Walling DE (1994) Using reservoir deposits to reconstruct changing sediment yields and
563 sources in the catchment of the Old Mill reservoir, South Devon, UK, over the past 50 years.
564 *Hydrolog Sci J* 39:347-368

565 Gallart F, Llorens P, Latron J, Regües D (2002) Hydrological processes and their seasonal controls in
566 a small Mediterranean mountain catchment in the Pyrenees. *Hydrol Earth Syst Sc* 6:527-537

567 Gumiere SJ, Raclot D, Cheviron B, Davy G, Louchart X, Fabre JC, Moussa R, Le Bissonnais Y.
568 (2011) MHYDAS-Erosion: a distributed single-storm water erosion model for agricultural
569 catchments. *Hydrol Process* 25:1717-1728

570 Gunal H, Ersahin S, Yetgin B, Kutlu T (2008) Use of chromameter measured color parameters in
571 estimating color related soil variables. *Commun Soil Sci Plan* 39:726-740

572 Jetten V, Boiffin J, De Roo APJ (1996) Defining monitoring strategies for runoff and erosion studies
573 in agricultural catchments: a simulation approach. *Eur J Soil Sci* 47:579-592

574 Jetten V, De Roo APJ, Favis-Mortlock D (1999) Evaluation of field-scale and catchment-scale soil
575 erosion models. *Catena* 37:521-541

576 Jetten V, Govers G, Hessel R (2003) Erosion models: quality of spatial predictions. *Hydrol Process*
577 17:887-900

578 López-Tarazón JA, Batalla RJ, Vericat D, Balasch JC (2010) Rainfall, runoff and sediment transport
579 relations in a mesoscale mountainous catchment: the River Isábena (Ebro basin). *Catena* 82:23-
580 34

581 Malam Issa O, Le Bissonnais Y, Planchon O, Favis-Mortlock D, Silvera N, Wainwright J (2006) Soil
582 detachment and transport on field- and laboratory-scale interrill areas: erosion processes and the
583 size-selectivity of eroded sediment. *Earth Surf Proc Land* 31:929-939

584 Mano V, Némery J, Belleudy P, Poirel A (2009) Assessment of suspended sediment transport in four
585 Alpine watersheds (France): influence of the climatic regime. *Hydrol Process* 23:777-792

586 Martínez-Carreras N, Udelhoven T, Krein A, Gallart F, Iffly JF, Ziebel J, Hoffmann L, Pfister L,
587 Walling DE (2010a) The use of sediment colour measured by diffuse reflectance spectrometry to
588 determine sediment sources: application to the Attert River catchment (Luxembourg). *J Hydrol*
589 382:49-63

590 Martínez-Carreras N, Krein A, Udelhoven T, Gallart F, Iffly JF, Hoffmann L, Pfister L, Walling DE
591 (2010b) A rapid spectral-reflectance-based fingerprinting approach for documenting suspended
592 sediment sources during storm runoff events. *J Soils Sediments* 10:400-413

593 Martínez-Carreras N, Krein A, Gallart F, Filia JF, Pfistera L, Hoffmann L, Owens PN (2010c)
594 Assessment of different colour parameters for discriminating potential suspended sediment
595 sources and provenance: A multi-scale study in Luxembourg. *Geomorphology* 118 (1-2):118-129

596 Mitas L, Mitasova H (1998) Distributed soil erosion simulation for effective erosion prevention. *Water*
597 *Resour Res* 34(3):505-516

598 Nadal-Romero E, Latron J, Martí-Bono C, Regüés D (2008) Temporal distribution of suspended
599 sediment transport in a humid Mediterranean badland area: the Araguás catchment, Central
600 Pyrenees. *Geomorphology* 97(3-4):601-616

601 Navratil O, Esteves M, Legout C, Gratiot N, Némery J, Willmore S, Grangeon T (2011) Global
602 uncertainty analysis of suspended sediment monitoring using turbidimeter in a small
603 mountainous river catchment. *J Hydrol* 398:246–259

604 Navratil O, Evrard O, Esteves M, Legout C, Ayrault S, Némery J, Mate-Marin A, Ahmadi M, Lefèvre
605 I, Poirel A, Bonté P (2012) Temporal variability of suspended sediment sources in an alpine
606 catchment combining river/rainfall monitoring and sediment fingerprinting. *Earth Surf Proc Land*
607 37:828-846.

608 Nearing MA (1998) Why soil erosion models over-predict small soil losses and under-predict large
609 soil losses? *Catena* 32:15–22

610 Owens PN, Batalla RJ, Collins AJ, Gomez B, Hicks DM, Horowitz AJ, Kondolf GM, Marden M,
611 Page MJ, Peacock DH, Petticrew EL, Salomons W, Trustrum NA (2005) Fine grained sediment
612 in river systems: environmental significance and management issues. *River Res Appl* 21:693-717

613 Phillips JD, Marion DA (2001) Residence times of alluvium in an east Texas stream as indicated by
614 sediment color. *Catena* 45:49-71

615 Pimentel D, Harvey CR, Resosudarmo P, Sinclair K, Kurz D, McNair M, Crist S, Shpritz L, Fitton L,
616 Saffouri R, Blair R (1995) Environmental and economics costs of soil erosion and conservation
617 benefits. *Science* 267:1117-1123

618 Poulénard J, Perette Y, Fanget B, Quetin P, Trevisan D, Dorioz JM (2009) Infrared tracing of
619 sediment sources in a small rural watershed (French Alps). *Sci Total Environ* 407:2808-2819

620 Poulénard J, Legout C, Némery J, Bramorski J, Navratil O, Douchin A, Fanget B, Perette Y, Evrard
621 O, Esteves M (2012) Tracing sediment sources during floods using Diffuse Reflectance Infrared

622 Fourier Transform Spectrometry (DRIFTS): A case study in a highly erosive mountainous
623 catchment (Southern French Alps). *J Hydrol* 414-415:452-462

624 Porta J. (1998) Methodologies for the analysis and characterization of gypsum in soils: a review.
625 *Geoderma* 87:31-46

626 Sánchez-Marañón M, Delgado G, Melgosa M, Hita E, Delgado R (1997) CIELAB color parameters
627 and their relationship to soil characteristics in Mediterranean soils. *Soil Sci* 162:833-842

628 Sánchez-Marañón M, Soriano M, Melgosa M, Delgado G, Delgado R (2004) Quantifying the effects
629 of aggregation, particle size and components on the colour of Mediterranean soils. *Eur J Soil Sci*
630 55:561-565

631 Slattery MC and Burt TP (1997) Particle size characteristics of suspended sediment in hillslope runoff
632 and stream flow. *Earth Surf Proc Land* 22:705-719

633 Soler M, Regues D, Latron J, Gallart F (2007) Frequency-magnitude relationships for precipitation,
634 stream flow and sediment load events in a small Mediterranean basin (Vallcebre basin, Eastern
635 Pyrenees). *Catena* 71(1):164-171

636 Takken I, Beuselinck L, Nachtergaele J, Govers G, Poesen J, Degraer G (1999) Spatial evaluation of a
637 physically based distributed erosion model (LISEM). *Catena* 37:431-447

638 Torrent J, Barron V (1993) Laboratory measurement of soil color: theory and practice. In: Bigham JM,
639 Ciolkosz EJ (eds) *Soil color*. Soil Science Society of America: Madison, Wisconsin, pp 21-34

640 Viscara Rossel RA, Walwoort DJJ, McBratney AB, Janik LJ, Skjemstad JO (2006) Visible, near
641 infrared, mid infrared or combined diffuse reflectance spectroscopy for simultaneous assessment
642 of various soil properties. *Geoderma* 131:59-75

643 Walling DE (2005) Tracing suspended sediment sources in catchments and river systems. *Sci Total*
644 *Environ* 344:159-184

645 Wang J, Bai SB, Liu P, Li YY, Gao ZR, Qu GX, Cao GJ. 2009. Channel sedimentation and erosion of
646 the Jiangsu reach of the Yangtze River during the last 44 years. *Earth Surf Proc Land* 34:1587-
647 1593

648 Wold S, Sjöström M, Eriksson L (2001) PLS-regression: a basic tool of chemometrics. *Chemometr*
649 *Intell Lab* 58(2):109-130

650 **List of figures**

651

652 **Fig. 1** Location of the Galabre catchment (a) with maps of the eroded areas, lithology and sampling
653 sites (b).

654 **Fig. 2** Artificial laboratory samples prepared by mixing the three source materials (i.e. black marls,
655 limestones and molasses) in controlled proportions.

656 **Fig. 3** Source material discrimination considering L^* and a^* parameters. The spectroscopic
657 measurements were taken on the $<63\text{-}\mu\text{m}$ size fraction. The number of collected source samples are in
658 parentheses.

659 **Fig. 4** Boxplot of the dispersed size fractions for suspended sediments and source material samples.
660 Black circles and white triangles correspond to outliers. The percentages were calculated considering
661 (a) the $<63\text{-}\mu\text{m}$ size fraction, (b) the $<31\text{-}\mu\text{m}$ fraction and (c) the $<16\text{-}\mu\text{m}$ fraction. The symbol * at
662 the end of each fraction label indicates that the two populations, i.e. suspended sediment and source
663 material, were significantly different according to the Dunn test.

664 **Fig. 5** Colorimetric parameter values for various size fractions of (a) molasses, (b) limestones and (c)
665 black marl samples. Gray circles indicate that measurements were significantly different from those
666 performed on the $<63\text{-}\mu\text{m}$ fraction according to Dunn test.

667 **Fig. 6** Various colorimetric parameter values with time spent in the river for (a) molasse, (b)
668 limestone and (c) black marl samples. Gray circles indicate that measurements were significantly
669 different from those taken after 1 day in the river according to the Dunn test.

670 **Fig. 7** Results of the partial least-squares regression models for (a) molasses, (b) limestones and (c)
671 black marls. Each model was constructed independently with the same set of 81 artificial laboratory
672 mixtures.

673 **Fig. 8** Predicted source material proportions in suspended sediment samples collected at the outlet of
674 the Galabre catchment using the partial least-squares regression models presented in Fig. 7. For each
675 of the 23 runoff events, a set of 5 to 23 suspended samples were collected during the event
676 and four measurements were conducted with the spectrophotometer on each sample (black
677 circles). The numbers above each group of four circles illustrate the temporal evolution of the
678 proportions of black marls and molasses during the 08/11/11 runoff event.

679 **Fig. 9** Comparison of the black marl proportions predicted by the partial least-squares regression
680 model presented in Fig. 7c and by other fingerprinting methods (Poulenard et al. 2012; Navratil et al.
681 2012). The samples were collected during the 22/11/07 and 12/08/08 runoff events. Error bars
682 correspond to the estimated uncertainty. The dashed line is the 1:1 line.

683 **List of tables**

684

685 **Table 1** Statistics of the absolute errors between actual and predicted proportions calculated using the
686 partial least-squares regression models presented in Fig. 7 detailed for each source material and for
687 various immersion durations in the river. Different letters given in brackets after the median
688 error indicate significant differences between immersion times according to the Dunn test.

689

690 **Table 2** Statistics of the absolute errors between actual and predicted proportions calculated using the
691 partial least-squares regression models presented in Fig. 7 detailed for each source material and for
692 various size fractions.

693

694 **Table 3** Statistics of the variations from one suspended sediment sample to the next collected during a
695 flood event of the predicted black marl proportion.

696

697

698 **Table 1** Statistics of the absolute errors between actual and predicted proportions calculated
 699 using the partial least-squares regression models presented in Fig. 7 detailed for each source
 700 material and for various immersion durations in the river. Different letters given in brackets
 701 after the median error indicate significant differences between immersion times according to
 702 the Dunn test.
 703

	Immersion time (days)	Number of samples	Median error (%)	1st quartile (%)	3rd quartile (%)
Black marl	0	12	1.7 (a b)	0.8	13.5
	7	36	2.8 (a b)	0.5	4.7
	14	36	1.2 (a)	0.5	4.0
	35	36	4.0 (b)	2.1	6.9
	63	36	2.5 (a b)	1.0	3.8
Molasse	0	12	12.9 (a)	5.0	15.9
	7	36	3.2 (b c)	1.6	5.0
	14	36	2.2 (c)	1.0	4.9
	35	36	6.0 (a)	2.4	9.2
	63	36	5.6 (a)	3.2	8.6
Limestone	0	12	3.8 (a)	3.2	12.3
	7	36	2.1 (b)	0.8	3.3
	14	36	0.5 (c)	0.3	1.5
	35	36	5.0 (a)	3.8	6.8
	63	36	4.4 (a)	2.4	6.6
All source samples	All immersion times	468	3.1	1.2	6.0

704
 705

706 **Table 2** Statistics of the absolute errors between actual and predicted proportions calculated
 707 using the partial least-squares regression models presented in Fig. 7 detailed for each source
 708 material and for various size fractions
 709

	Size fraction (μm)	Number of samples	Median error (%)	1st quartile (%)	3rd quartile (%)
Black marl	<200	20	15.3	12.5	21.7
	<100	20	15.6	8.1	20.2
	<63	20	2.7	1.5	12.8
	<20	20	5.5	3.8	14.8
Molasse	<200	20	19.3	14.6	24.5
	<100	20	16.7	11.3	24.4
	<63	20	5.4	1.8	18.3
	<20	20	11.1	8.9	17.3
Limestone	<200	20	1.9	0.7	5.9
	<100	20	1.9	0.8	3.6
	<63	20	3.0	1.6	3.9
	<20	20	7.7	6.0	12.9
All source samples	<63	60	3.3	1.8	16.6
All source samples	All sizes except <63 μm	180	11.5	4.2	19.4

710
 711

712 **Table 3** Statistics of the variations from one suspended sediment sample to the next collected
 713 during a flood event of the predicted black marl proportion.

714

Runoff event	Number of samples with variation > 50%	Mean variation (%)	Std. Dev. (%)	Range (%)
03/05/11	0	3	4	7
14/10/08	0	0	1	3
22/11/07	1	11	15	42
11/01/08	1	13	13	39
29/05/08	1	11	18	76
12/08/08	1	5	15	60
03/03/09	1	13	8	21
14/12/10	1	13	22	46
30/05/11	1	9	24	68
18/06/08	3	11	27	81
19/09/08	2	6	16	58
31/10/08	6	46	40	100
19/11/08	5	46	47	106
24/06/10	2	34	42	98
15/09/10	3	25	40	110
10/11/10	2	19	20	50
09/06/11	4	25	33	84
05/07/11	2	85	4	5
19/07/11	3	12	28	87
30/08/11	2	18	41	92
28/09/11	2	8	19	60
08/11/11	9	39	33	91

715
 716

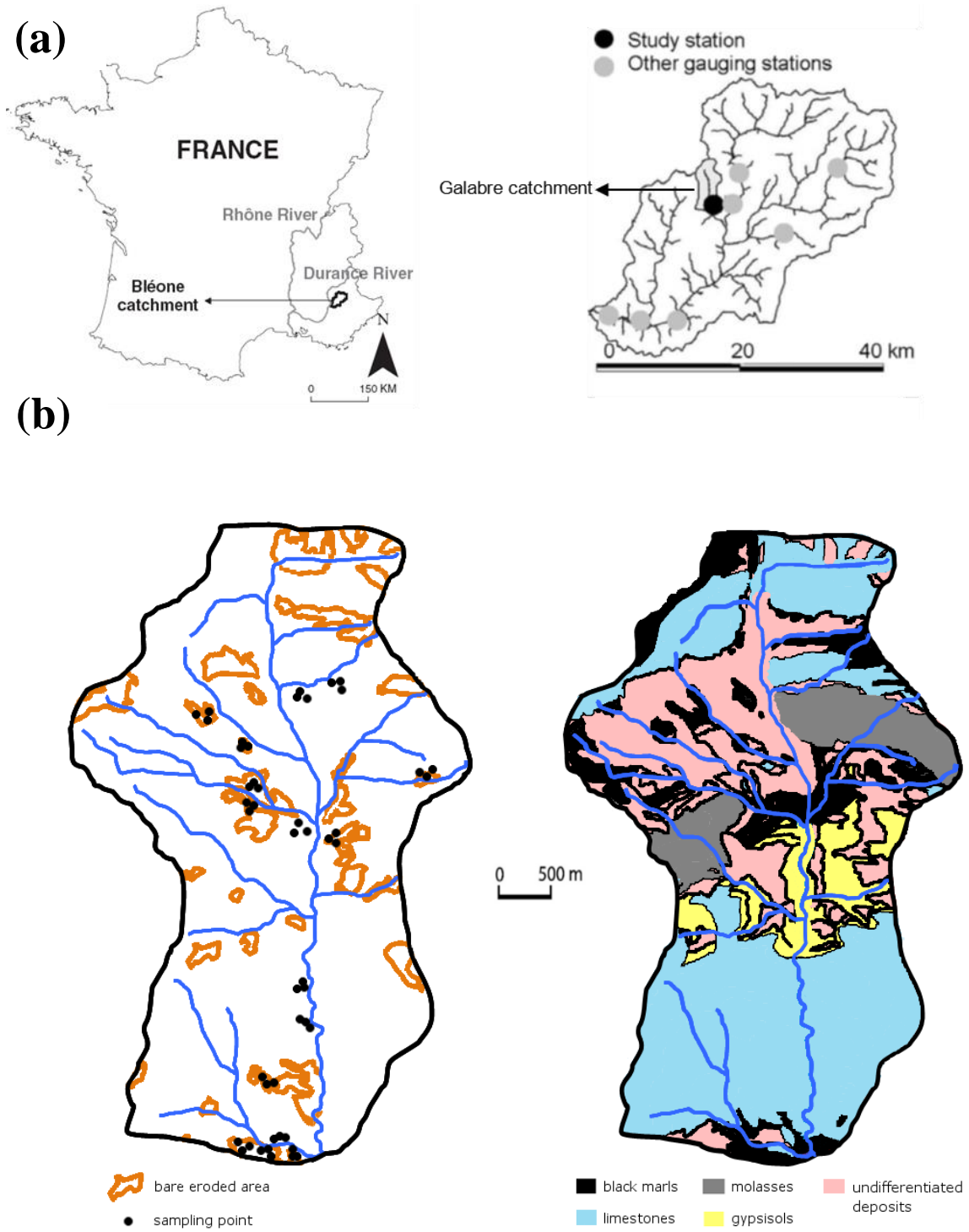


Fig. 1 Location of the Galabre catchment (a) with maps of the eroded areas, lithology and sampling sites (b).

717

718

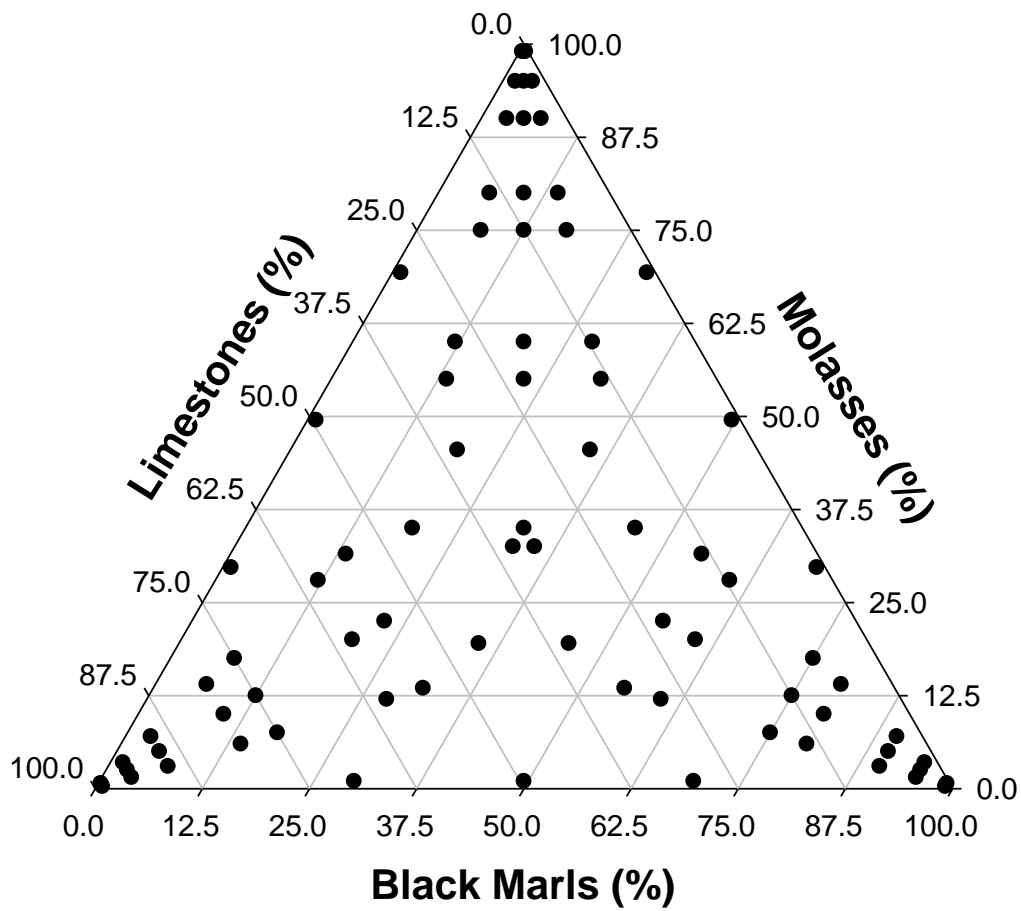


Fig. 2 Artificial laboratory samples prepared by mixing the three source materials (i.e. black marls, limestones and molasses) in controlled proportions.

719

720

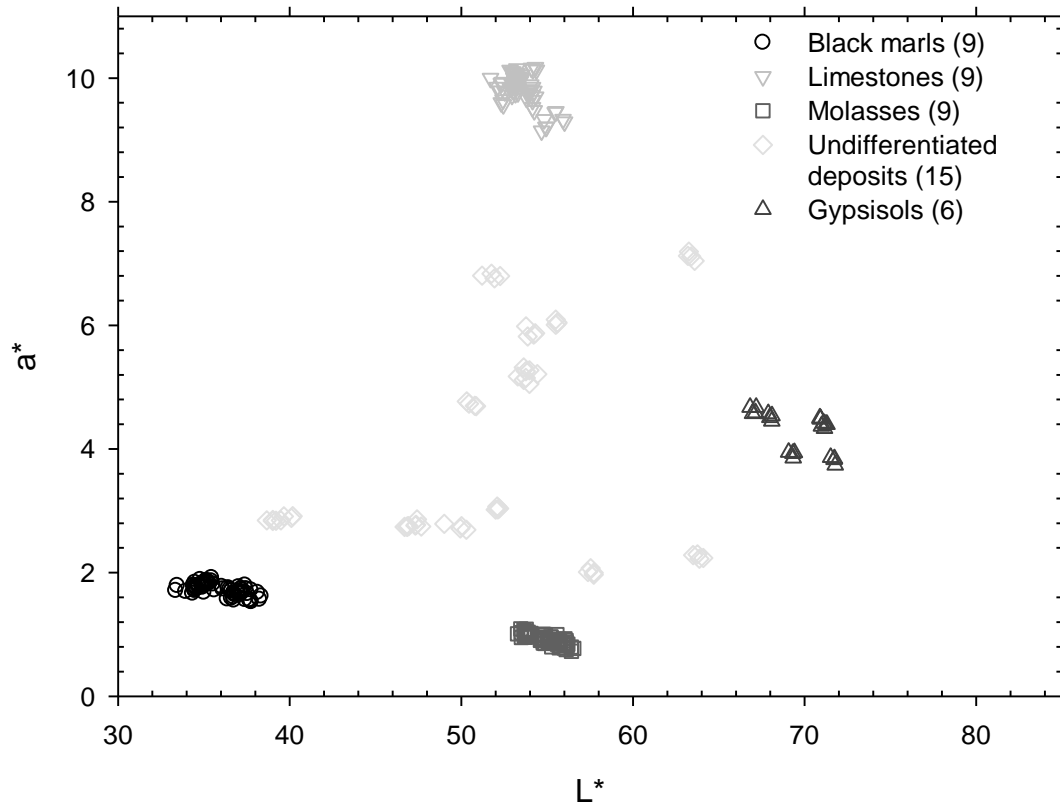
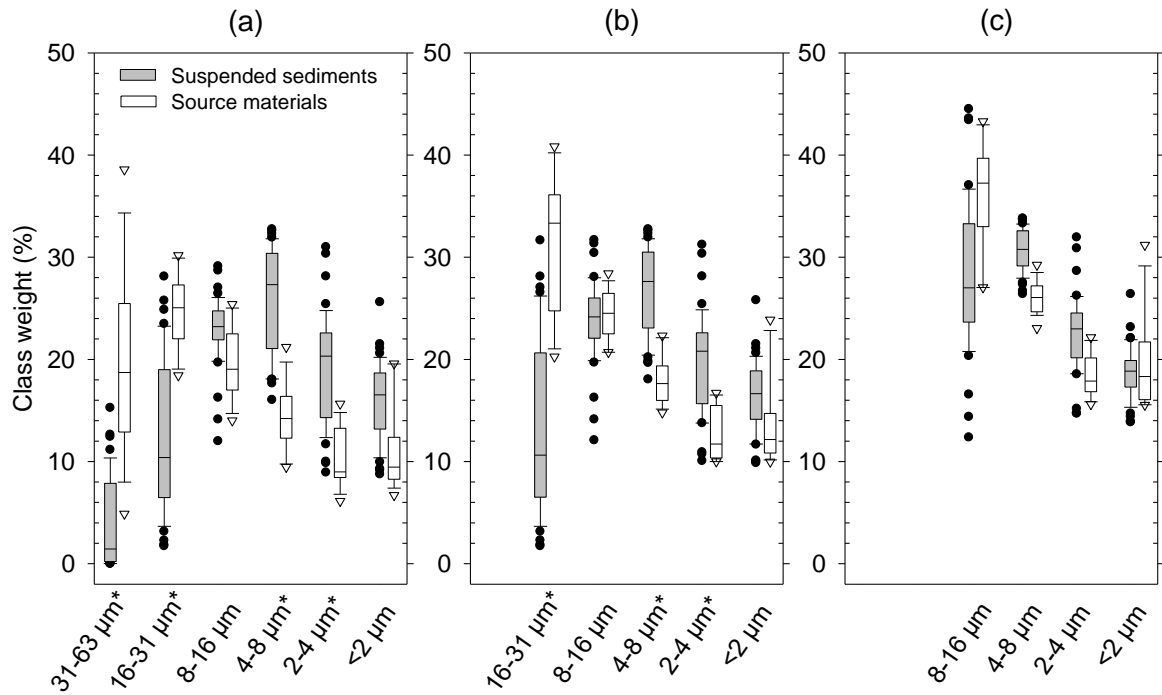


Fig. 3 Source material discrimination considering L^* and a^* parameters. The spectroscopic measurements were taken on the $<63\text{-}\mu\text{m}$ size fraction. The number of collected source samples are in parentheses.

721

722



723
724

Fig. 4 Boxplot of the dispersed size fractions for suspended sediments and source material samples. Black circles and white triangles correspond to outliers. The percentages were calculated considering (a) the <63- μm size fraction, (b) the <31- μm fraction and (c) the <16- μm fraction. The symbol * at the end of each fraction label indicates that the two populations, i.e. suspended sediment and source material, were significantly different according to the Dunn test.

725
726

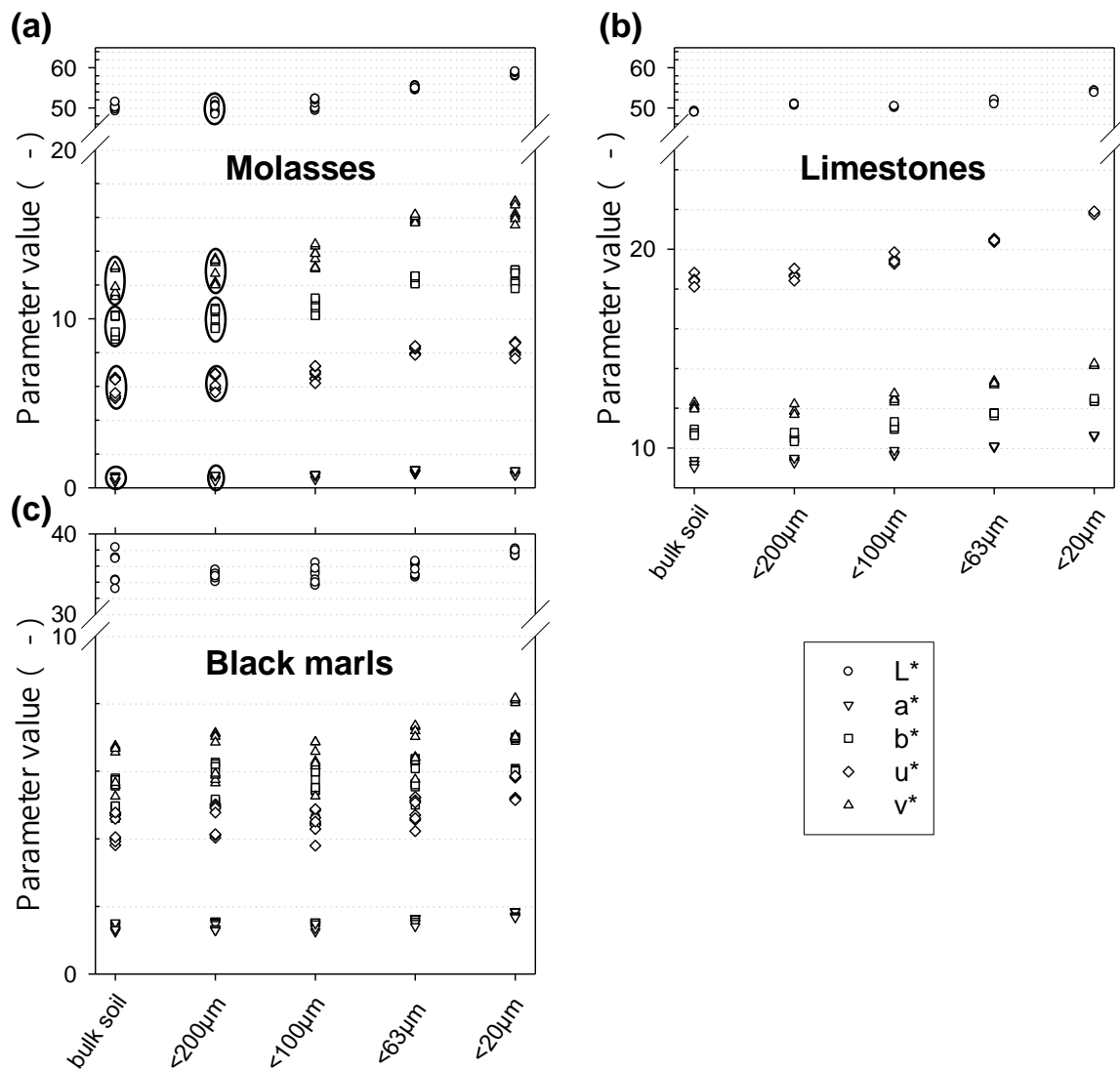


Fig. 5 Colorimetric parameter values for various size fractions of (a) molasses, (b) limestones and (c) black marl samples. Gray circles indicate that measurements were significantly different from those performed on the <63-µm fraction according to Dunn test.

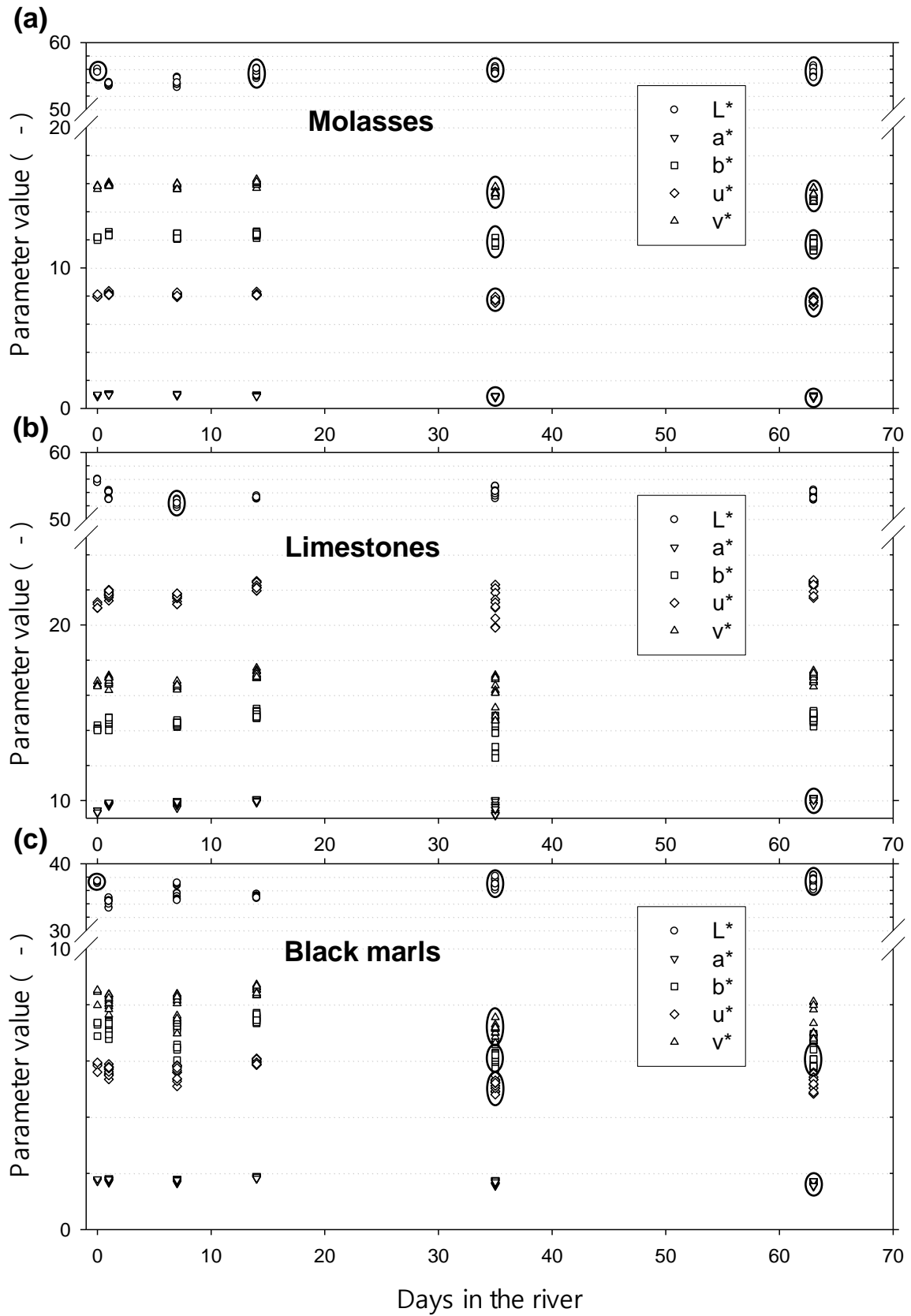


Fig. 6 Various colorimetric parameter values with time spent in the river for (a) molasse, (b) limestone and (c) black marl samples. Gray circles indicate that measurements were

significantly different from those taken after 1 day in the river according to the Dunn test.

728

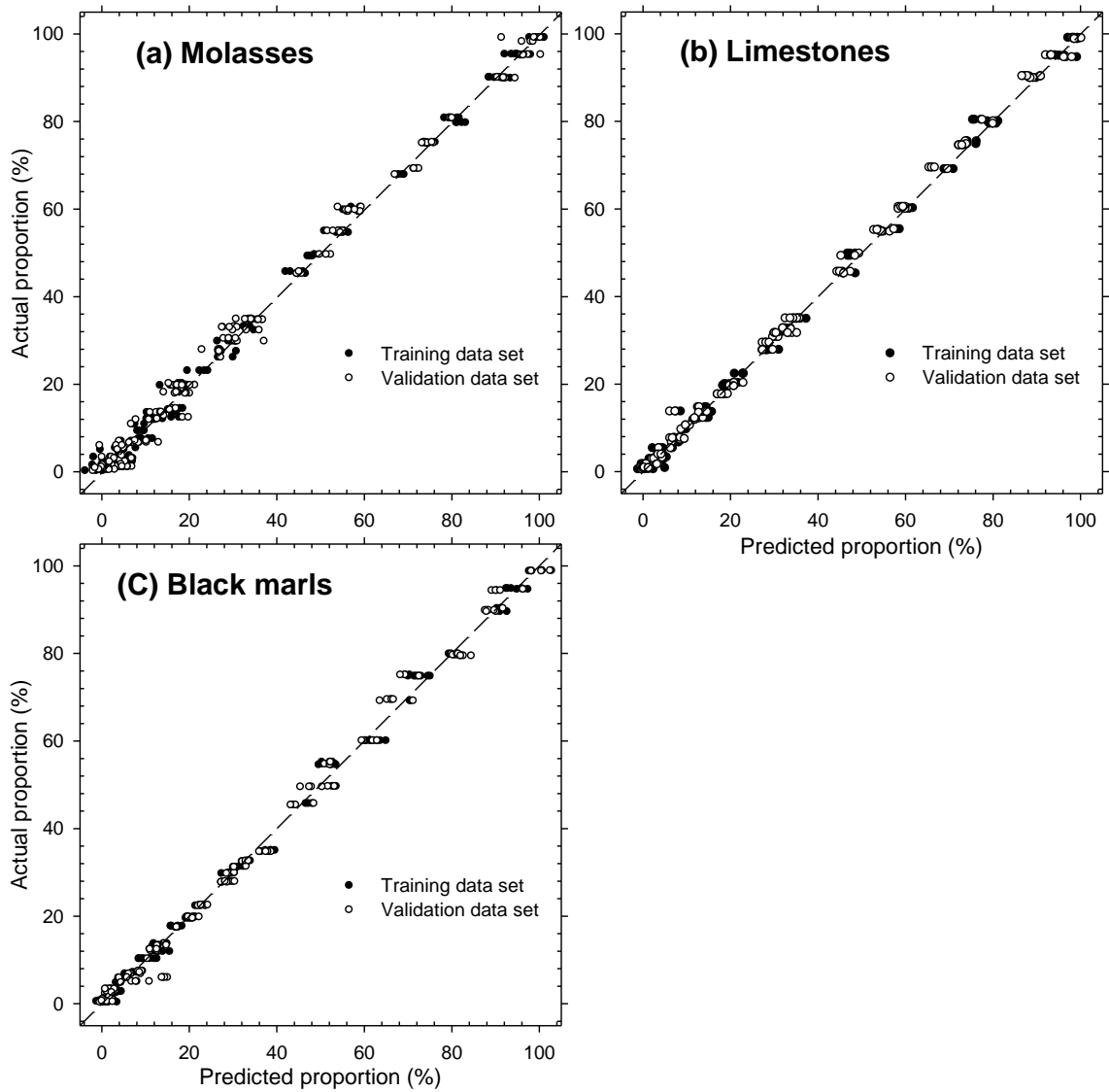


Fig. 7 Results of the partial least-squares regression models for (a) molasses, (b) limestones and (c) black marls. Each model was constructed independently with the same set of 81 artificial laboratory mixtures.

729

730

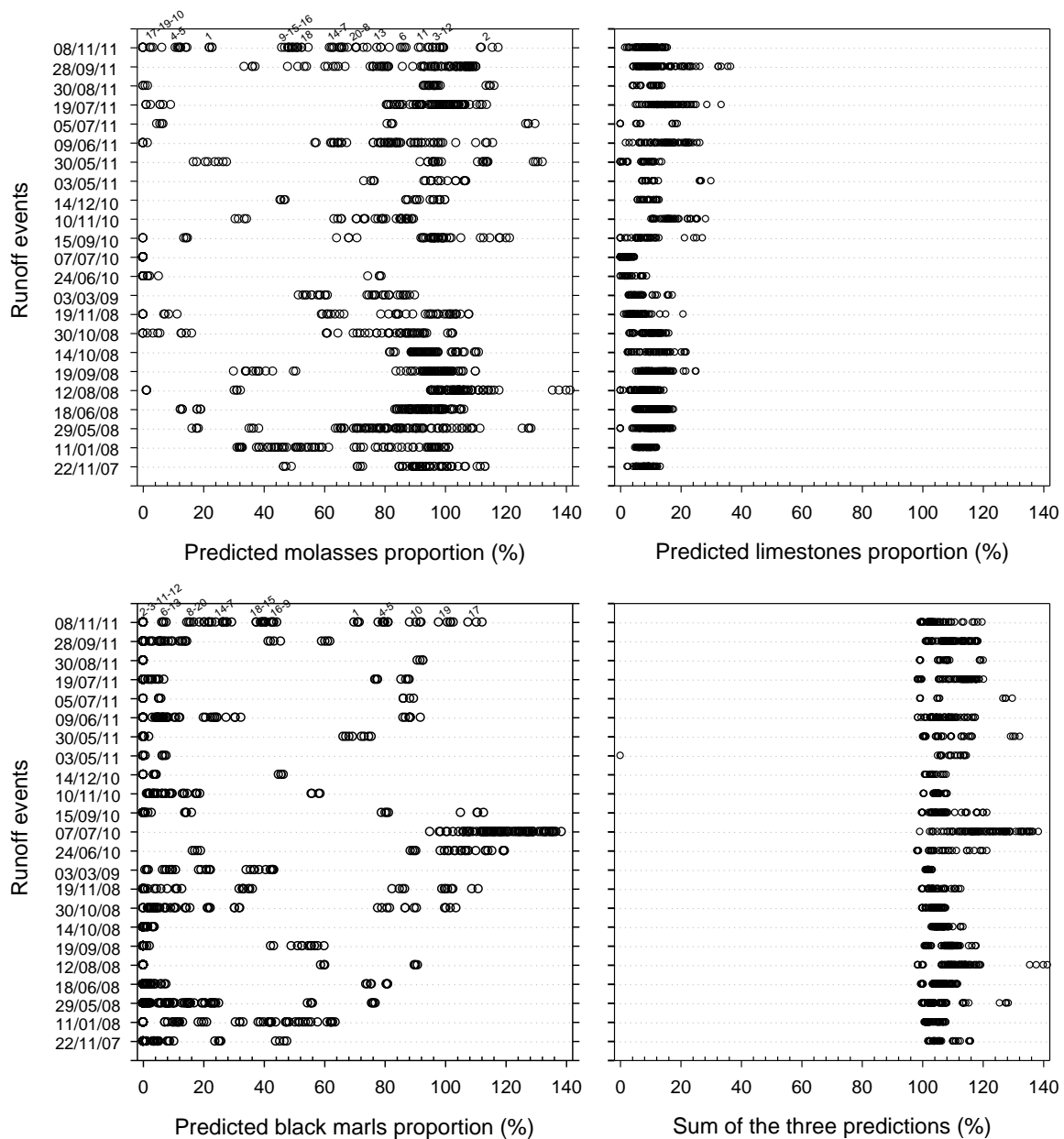


Fig. 8 Predicted source material proportions in suspended sediment samples collected at the outlet of the Galabre catchment using the partial least-squares regression models presented in Fig. 7. For each of the 23 runoff events, a set of 5 to 23 suspended samples were collected during the event and four measurements were conducted with the spectrophotometer on each sample (black circles). The numbers above each group of four circles illustrate the temporal evolution of the proportions of black marls and molasses during the 08/11/11 runoff event.

731

732

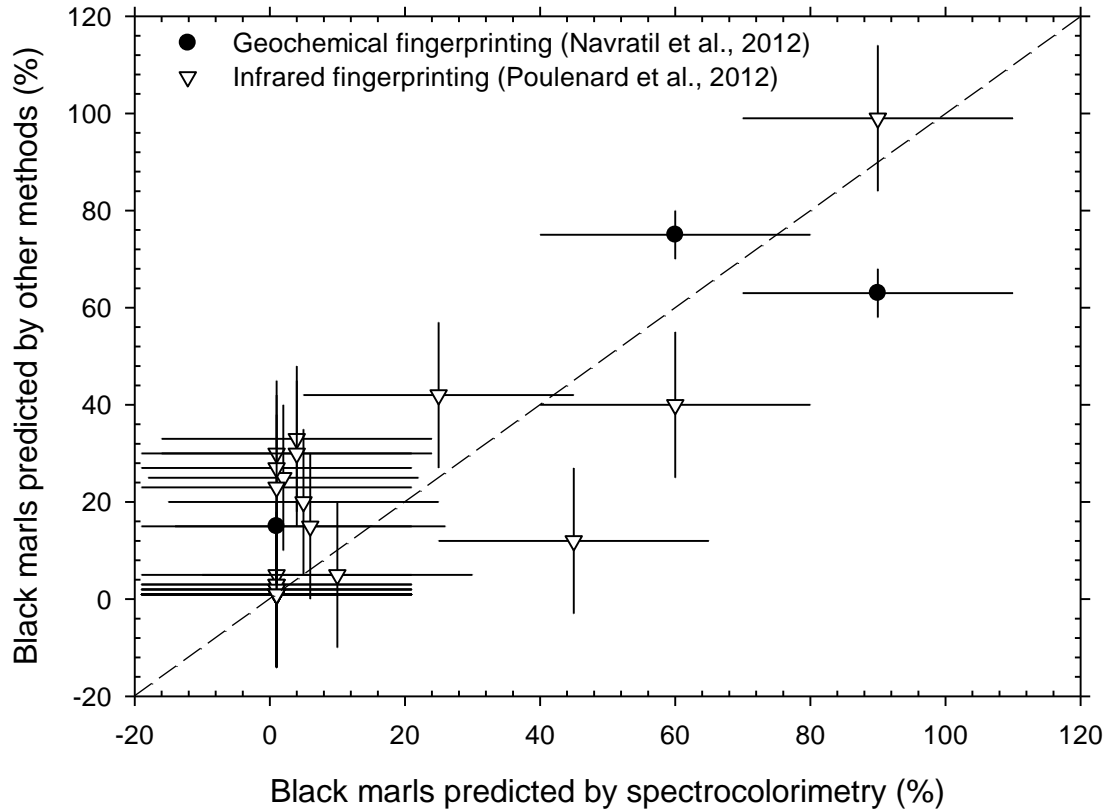


Fig. 9 Comparison of the black marl proportions predicted by the partial least-squares regression model presented in Fig. 7c and by other fingerprinting methods (Poulenard et al. 2012; Navratil et al. 2012). The samples were collected during the 22/11/07 and 12/08/08 runoff events. Error bars correspond to the estimated uncertainty. The dashed line is the 1:1 line.